

EXPERIMENTAL DESIGN OF AN ACTIVE ANTENNA FOR
RADIO FREQUENCY IDENTIFICATION APPLICATION

A Senior Thesis

By

Michael A. Saville

1996-97 University Undergraduate Research Fellow

Texas A&M University

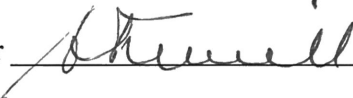
Group: ENGINEERING

Experimental Design of an Active Antenna for
Radio Frequency Identification Applications

Michael A. Saville
University Undergraduate Fellow, 1996-97
Texas A&M University
Department of Electrical Engineering

APPROVED

Fellows Advisor 

Honors Director 

Abstract

Experimental Design of an Active Antenna for
Radio Frequency Identification Applications (April 1997)
Michael A. Saville, Texas A&M University
Advisor: Dr. Kai Chang

Radio frequency identification (RFID) is the process of acquiring information by use of electromagnetic energy. These systems are completely noncontact and often utilize microwave components. The need for smaller components, less cost, and lower power consumption make the active antenna well suited for this application.

This study attempts to develop a planar, FET based integrated active antenna for RFID applications. First a passive microstrip ring antenna is developed for integration with a nominal 50 ohm output oscillator. The antenna exhibits a 70 degree beamwidth in the E-plane with a -18 dB down cross-pol and an 80 degree beamwidth in the H-plane with a -30 dB down cross-pol. The return loss is -28.5 dB into 50 ohms. Second, a 5.8 GHz oscillator design is explored using S-parameter techniques and CAD simulations. Although the initial design does not meet specifications for integration with the microstrip ring antenna, the experimental results later verify the accuracy of the CAD simulations. This study concludes with an analysis of active antenna measurements based on the continued research to develop the oscillator for integration with the microstrip ring antenna.

To my wife Deysi, our son Michael, and our daughter Kristen.

ACKNOWLEDGMENTS

I would like to thank Dr. Kai Chang for inviting me to accept this project. I would also like to thank Mr. Lu Fan for sharing his numerous ideas and always providing assistance in the lab.

Finally, I would like to thank all of the microwave lab graduate students, research assistants, and visiting professors for helping out in the lab and keeping me straight with the theory.

TABLE OF CONTENTS

SECTION	Page
ABSTRACT.....	ii
DEDICATION.....	iii
ACKNOWLEDGEMENTS.....	iv
TABLE OF CONTENTS.....	v
LIST OF FIGURES.....	vii
I INTRODUCTION	1
A. RFID Systems.....	1
B. RIC VS. RFID.....	2
C. Why Active Antennas?.....	2
D. Objective of this study.....	3
II MICROSTRIP ACTIVE ANTENNAS.....	3
A. Active microstrip antennas.....	3
III MICROSTRIP RING ANTENNA.....	7
A. Microstrip ring theory.....	7
B. Microstrip ring design.....	11
C. Antenna testing.....	13
D. Experimental results.....	17
IV OSCILLATOR DESIGN.....	20
A. Oscillator theory.....	20
B. Oscillator testing.....	22
C. Oscillator experiments.....	23
V INTEGRATED ACTIVE ANTENNA RESULTS.....	27
A. Integrated active antenna measurements.....	27

VI CONCLUSIONS.....	29
REFERENCES.....	30
APPENDIX A.....	A-1
APPENDIX B.....	B-1

LIST OF FIGURES

FIGURE		Page
1	Conventional and active antenna.....	3
2	Oscillation conditions for two terminal device with load.....	5
3	Typical I-V curve for a Gunn diode.....	5
4	Rectangular patches with Gunn diode.....	6
5	Microstrip ring circuit.....	8
6	Coupled microstrip feed and probe feed.....	10
7	Two port network with incident and reflected voltages.....	11
8	Theoretical return loss obtained from IE3D simulation.....	12
9	Antenna radiation pattern test set-up.....	14
10	Measured return loss of microstrip ring antenna.....	18
11	Radiation pattern.....	19
12	Two port oscillator design model.....	21
13	Oscillator output impedance from Libra simulation.....	24
14	Measured oscillator power spectrum.....	25
15	Measured fundamental frequency stability.....	26

I. Introduction

A. RFID Systems

Radio Frequency Identification (RFID) Systems date back to the early years of air traffic control radar identification systems [1]. The Interrogate Friend or Foe (IFF) radar systems would transmit an electromagnetic signal to an unidentified aircraft that carried a transceiver, or transponder. The transponder would then reply with a coded electromagnetic signal that could be decoded and used by ground controllers for identification purposes.

Later, these systems were developed for smaller, light-weight, and less expensive identification applications, such as animal tracking, asset tagging, security products, access control, and transportation uses [1]. Unlike bar code labeling, transponders, or tags, do not need a line of sight for clear transmission. They are also non-contact as opposed to magnetic labeling. However, there are difficulties for mass producing RFID tags.

The main problems that prevent a wide scale application of RFID tags are cost, and standardization [1], [2]. Tags range in price from \$1 to \$60 dollars, and can cost considerably more for read and write tags. The latter allow changes to the tags' stored information through electromagnetic radio communication. The primary reason for the wide range of costs is the diversity of the applications. Tags are classified into active, passive, or transponder devices. Active tags use their own power source and develop their own radio frequency (RF) signal. The power source is usually a battery, and the tags can be designed for continuous or periodic transmission. Passive tags may still use a battery for storing digital information, but they do not generate their own RF signal. Transponder tags are passive, but they utilize the incident RF power (interrogator signal) to turn on their circuitry and generate an RF signal.

Standardization is difficult because of the numerous RFID applications. Each application has its own restrictions. These include working distance, tag-to-tag spacing, power source, data length, data integrity, tag size, tag shape, tag cost, ruggedness, and reliability [2], [3]. In addition, there are many manufacturers of RFID systems that don't accept the same standard, and therefore have incompatible systems. Internationally standardization is also an issue. Japan, Germany, South Korea, and Brazil use different systems, with Brazil using three different systems alone. For the RFID system designer, the challenge is to design an adaptable standard for use with many different systems.

B. RIC VS. RFID

In addition to cost and adaptability concerns are small size, low power, and memory requirements. These needs have paved the way for a new breed of RFID components. These components, called Remote Intelligent Communication (RIC) systems, are integrated circuits that include a receiver, a modulator, a clock system, and a microcontroller. Micron Communications Inc. recently developed the MicroStamp unit, which when combined with a battery and an antenna, forms the MicroStamp RIC unit [4]. The main difference between the RFID and RIC technologies are the expanded capabilities of RIC vs. RFID. RIC incorporates digital signal processing circuits, more memory, and low power integrated circuit operation. Although these new devices have enhanced capabilities, the need for smaller components, lower power consumption, and lower cost, still drive the research. This is what the active antenna offers.

C. Why Active Antennas?

Active antenna systems differ from conventional transceiver systems by using an active component directly integrated on the antenna, or at the antenna terminals. Figure 1, taken from

[5], shows a conventional approach where the transitions transfer power from the component to a transmission line, and from the transmission line to the antenna. The added components result in larger size, higher loss, and greater cost. Figure 1b, shows the active antenna approach which eliminates the transitions and transmission line.

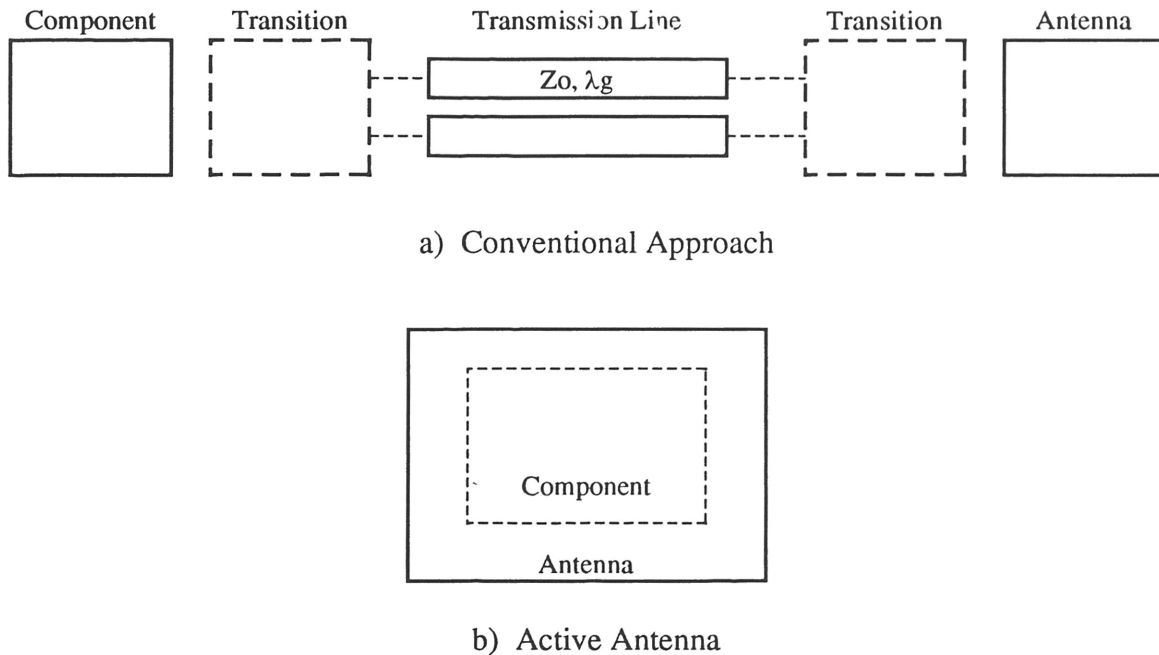


Figure 1. Conventional and active antenna.

Although there are advantages to the active antenna, there are difficulties as well. The first is the design. Conventional systems are designed by selecting the components and using intermediate networks and components to connect them in a system. Each component is designed apart from the other components. With the active antenna, the active component and the antenna must be designed as one unit. This adds complexity to the design and analysis. Also, they are usually designed for a specific application which limits their usefulness.

There are many different types of antennas that can be used in microwave systems. However, RFID tag antennas are limited to planar construction such as printed antennas for low

cost, small size and conformable nature [6]. Microstrip was selected for this study because of its mature theory, low cost, and repeatability. Additional considerations for the antenna are the active solid-state device components. They must meet certain restrictions such as size, power efficiency, and cost.

D. Objective of this study.

This study looks at different active antennas developed for wireless communication systems, and attempts to develop a planar field effect transistor (FET) based active antenna for RFID systems. The second section discusses these various design considerations for active antennas. The third and fourth sections of this thesis show the antenna and oscillator designs as separate components. Traditional design techniques are used to provide a baseline for studying the integration of the two components in section V. Finally, section VI provides conclusions for the effectiveness of this active antenna, and examines the merits of the active antenna as it applies to RFID systems.

II. Microstrip Active Antennas

A. Active microstrip antennas.

There are many types of active antennas and they are often sorted into two basic groups, transmitters and receivers. However, a simple classification method is to sort them by the type's of function's performed by the active device [7]. The devices may generate RF power, amplify, or convert frequencies. The function of the RFID active component is to generate microwave frequencies. This may be either a frequency tunable oscillator or a single frequency source

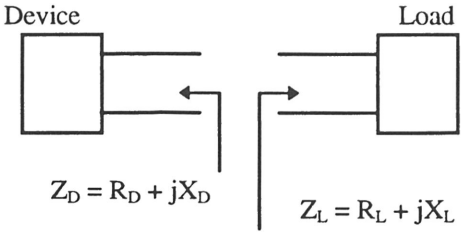
Some of the considerations for the oscillator are the quality factor (Q-factor), stability, AM and FM noise, and load pulling. The quality factor depends on different losses in the circuit. A higher Q-factor means more energy is stored in the circuit than is lost in the circuit per cycle of oscillation. This results in better stability. The stability determines how well the oscillator returns to a steady state condition after some disturbance, such as thermal, electrical, or mechanical disruptions. Noise consists of random amplitude and phase variations. There are complex models for calculating oscillator noise [7], but it is difficult to take them into account. Pulling is the tendency of the oscillator to drift with load fluctuations.

Different devices have characteristics that can be used for oscillation. Gunn diodes are very popular because they are two terminal devices and are easily made to oscillate. However, the Gunn diode demands larger voltage and current than other devices for oscillation, and often have higher noise. Field effect transistors (FETs) are three terminal devices, which complicate the circuit, but they operate with much lower voltage and current. Also, microwave devices such as metal to semiconductor FETs (MESFETs) often have lower noise values and work well as stable oscillators. When integrated into an active antenna, the antenna serves as the resonant structure for the oscillator as well as the load. Any oscillator must meet two conditions before oscillation will start:

- 1) the device must exhibit a negative resistance, and
- 2) the circuit reactance must be zero.

Figure 2 shows a two terminal device and the load with the conditions for oscillation. The device is placed on the antenna in a position that satisfies the second condition, and the operating voltage

and current for the device are used to ensure that condition one is satisfied. A typical Gunn diode voltage vs. current plot is shown in Figure 3.



Oscillation Conditions

$|R_D| > R_L$ (1),

$X_D = -X_L$ (2)

Figure 2. Oscillation Conditions for two terminal device with load.

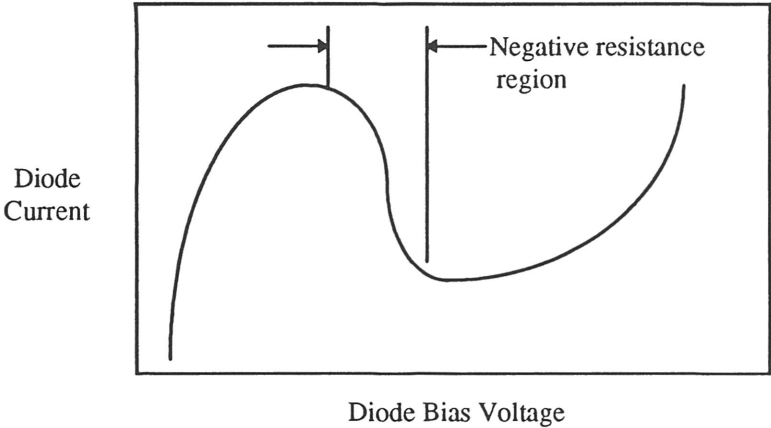


Figure 3. Typical I-V curve for a Gunn diode.

Recall that the device resistance is defined as the slope of the I-V curve. The plot shows how the device’s negative resistance can be changed by tuning the bias voltage. Subsequently, the frequency is tuned because the device’s impedance changes with the voltage. For some RFID

applications a frequency modulation scheme can be employed by changing the device's bias with the information signal.

A cavity backed Gunn diode driven circular patch antenna developed by Montiel et al. [8], demonstrated a 6 GHz RF source with a 200 MHz bias tuning range. The diode was placed on the patch for best radiation pattern and the cavity size was tuned for a final circuit reactance equal to zero at this frequency. Another cavity backed circular patch antenna, implemented with a MESFET, achieved a 287 MHz tuning range at 5.8 GHz, with a 19% dc to RF efficiency [9]. Although, the bias tuning ranges are small (3-5%), the ranges are easily increased up to 13% by adding a varactor to the circuits [8].

The MESFET offers a much higher dc to RF efficiency than Gunn diodes, which is an important requirement for RFID applications [10]. Planar designs for active antennas allow possibilities for RFID tag applications. Some planar designs include modulated backscatter approaches with mixer diodes, [11], and modified rectangular patches. Rectangular patches shown in Figure 4b were used to match a Gunn diode to the patch with higher spectral purity and lower cross polarization levels than the reference active patch antenna [10]. Optimal matching is achieved by changing the width and length of the stub and the radiation pattern is only slightly affected.

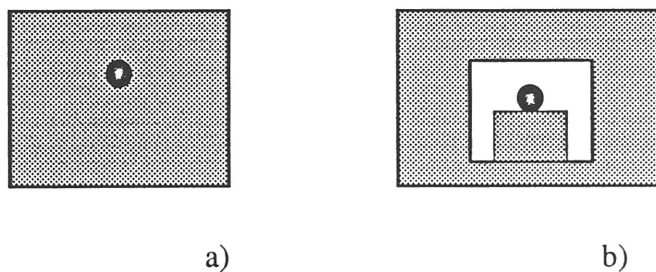


Figure 4. Rectangular patches with Gunn diode a) Reference Patch b) Modified patch

These patches are not uniplanar in design because the Gunn diode must be mounted in the substrate which requires drilling a hole through the substrate. Also the FETs are often configured as two port networks which require drilling one terminal to ground. A completely uniplanar slotline ring antenna was introduced by Ho et al. [12]. The slotline structure is completely uniplanar which means that the single FET is easily mounted on the device. The active antenna radiated 21.6 mW with 18% dc to RF efficiency [12]. One unique characteristic of the ring is the smaller size than those of circular and rectangular patches.

The FET offers small size, low power, and low noise, and the ring antenna offers small size with various methods for integration with the FET. The next section describes the ring antenna design and experiments.

III. Microstrip Ring Antenna

A. Microstrip ring theory.

The microstrip ring antenna differs from the microstrip ring resonator by the width of the microstrip line and the mode of operation. Figure 5 shows a microstrip ring antenna, where h is the substrate height, ϵ_r is the relative dielectric constant for the substrate, and w is the width of the microstrip line that forms the ring. Different substrates may be used, and each has a different value of ϵ_r .

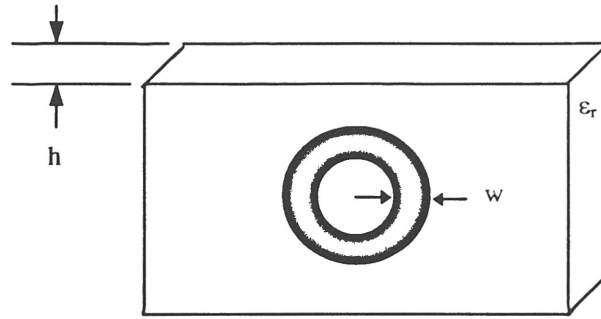


Figure 5. Microstrip ring circuit.

Microstrip rings support TM_{mn} modes, and the TM_{12} mode was shown to be the best mode of operation for the ring antenna as opposed to the TM_{11} mode for ring resonators [12]. Resonance for the antenna is established when the mean circumference of the ring is equal to an integral multiple of a guided wavelength.

$$2\pi r = n\lambda_g \quad (3),$$

where r is the mean radius, n is the mode number, and λ_g is the guided wavelength. Additional considerations are microstrip dispersion for a ring and the feed line to the ring.

Microstrip dispersion results in different velocities of the electromagnetic waves propagating on the microstrip line. Essentially, the physical circuit size is affected so the change is characterized as an effective relative dielectric constant in the same way that the relative dielectric constant relates to a free space medium.

$$\lambda_g = \frac{\lambda_0}{\sqrt{\epsilon_r}} \quad (4),$$

$$\lambda_{g,eff} = \frac{\lambda_g}{\sqrt{\epsilon_{r,eff}}} \quad (5),$$

where λ_o is the free space wavelength, λ_g is the guided wavelength in a medium other than free space, and $\lambda_{g,eff}$ is the effective guided wavelength.

Dispersion effects are well documented with accurate results. Chang shows a simple method to determine the radius of the ring, which includes dispersion effects [13]; a well known microwave circuit design program called *LineCalc* [14] is used to determine the width for a 50 ohm microstrip line when given the substrate thickness and dielectric constant. The effective dielectric constant, and guided wavelength are then computed with the microstrip dispersion equation, (6), developed by Kirshing and Jansen [15].

$$\epsilon_{eff} = \epsilon_r - \frac{\epsilon_r - \epsilon_c}{1 + P(f)} \quad (6),$$

where f is the frequency in GHz, ϵ_r is the relative dielectric constant for the substrate, ϵ_c is the static value of the effective dielectric constant, and $P(f)$ is a frequency dependent function based on the microstrip line width, substrate height, and microstrip geometry.

The type of feed commonly used for a ring antenna is a probe feed. This is because a device such as a Gunn diode can be placed in the substrate similar to a probe being attached to the conducting ring. However, this type of design doesn't allow any post fabrication tuning because once placed the device can not be moved. This is an experimental study so alternate feeds are considered. Microstrip resonators often use coupled lines and this allows control over the power absorbed by the resonator. The microstrip coupled line allows post fabrication tuning of the resonant frequency with microstrip stub tuners. A tuning stub can be appropriately placed along the microstrip line to change the input impedance of the antenna, thereby changing the resonant frequency. Figure 6 shows the coupled feed line and probe feed.

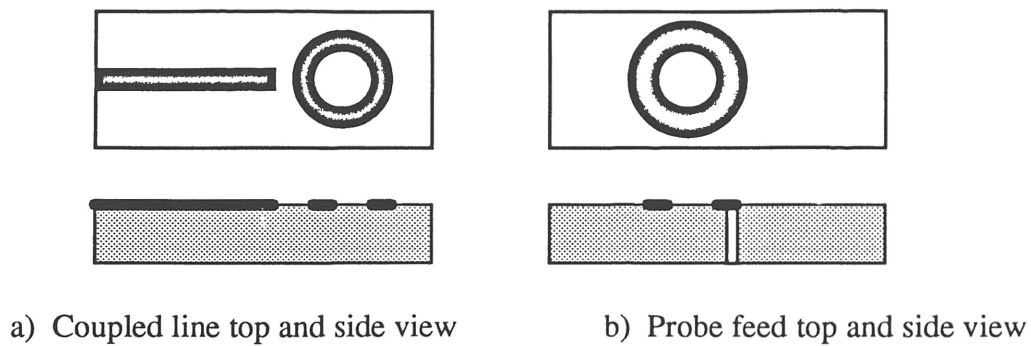


Figure 6. Coupled microstrip feed and probe feed.

A microstrip line can directly feed the ring antenna, but the FET DC bias lines begin to complicate the circuit, and deteriorate the power pattern.

Any antenna is described by its electric field, and its magnetic field. Together, they are used to determine the power radiation pattern and antenna gain. The ring antenna, fed with a current that is transverse to the antenna, has electric and magnetic fields described by equations (7) and (8), [13].

$$E_z(\rho) = A_n J_n(k\rho) + B_n Y_n(k\rho) \quad (7),$$

$$H_\phi(\rho) = -\frac{jk}{\omega\mu_0} [A_n J'_n(k\rho) + B_n Y'_n(k\rho)] \quad (8),$$

where ρ is the radial distance from the center of the patch along the surface of the antenna, k is the phase constant in radians per meter, $J_n(k\rho)$ is the n th order Bessel function, $Y_n(k\rho)$ is the n th order Neumann function, $J'_n(k\rho)$ is the derivative of the n th order Bessel function, and $Y'_n(k\rho)$ is the derivative of the n th order Neumann function. A_n and B_n are arbitrary constants. The subscripts z , and ρ refer to a cylindrical coordinate system with the z -axis through the substrate.

The input impedance of a probe fed ring antenna was derived by Bhattacharyya, and Garg, [16], [17], based upon a radial transmission line model. MathCad was used to simulate the

published results, [16], [17], so that the ring could be impedance matched to an FET directly. However, a coupled line was used to feed the antenna, so this model was not used.

B. Microstrip ring design.

The ring design is shown in Appendix A. 5.8 GHz was selected as the design frequency because it is in the unlicensed Industrial, Scientific, and Medical band, and is often used for RFID applications [2]. The microstrip substrate is Duroid 6010 with a 50 mil thickness, and a dielectric constant of 10.5. The full wave electromagnetic simulator, *IE3D* [18], was used to analyze the microstrip ring structure with the moment method. This program returns the scattering parameters which can then be used to calculate the circuit return loss.

Scattering (S-) parameters are used with multi-port microwave networks to determine power reflected and transmitted. Figure 7. shows the S-parameters for a two port network.

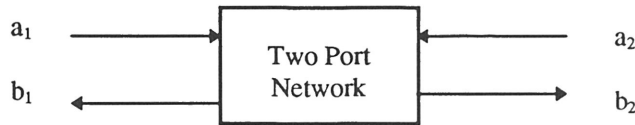


Figure 7. Two port network with incident and reflected voltages.

Energy into the network is denoted with a_1 , and a_2 , while energy output from the network is represented with b_1 , and b_2 . The S-parameters are defined as the ratio of incident energy to reflected energy. They are measured with energy input into one port while the other port is impedance matched to a standard 50 ohm load. This gives the following relationship for the four S-parameters in a two port network.

$$S_{11} = b_1 / a_1 \quad (9),$$

$$S_{12} = b_1 / a_2 \quad (10),$$

$$S_{21} = b_2 / a_1 \quad (11),$$

$$S_{22} = b_2 / a_2 \quad (12),$$

where a and b are in volts, and the S-parameter subscripts refer to energy reflected due to energy incident (for S_{11} and S_{22}), and energy transmitted due to energy incident (for S_{21} and S_{12}).

The ring antenna is a one port device, so only the scattering parameter, S_{11} , is used to check the resonant frequency of the antenna. S_{11} is plotted vs. frequency on a decibel scale in Figure 8. The narrow dip at 6.05 GHz shows minimum returned power, thus the circuit is resonant at this frequency.

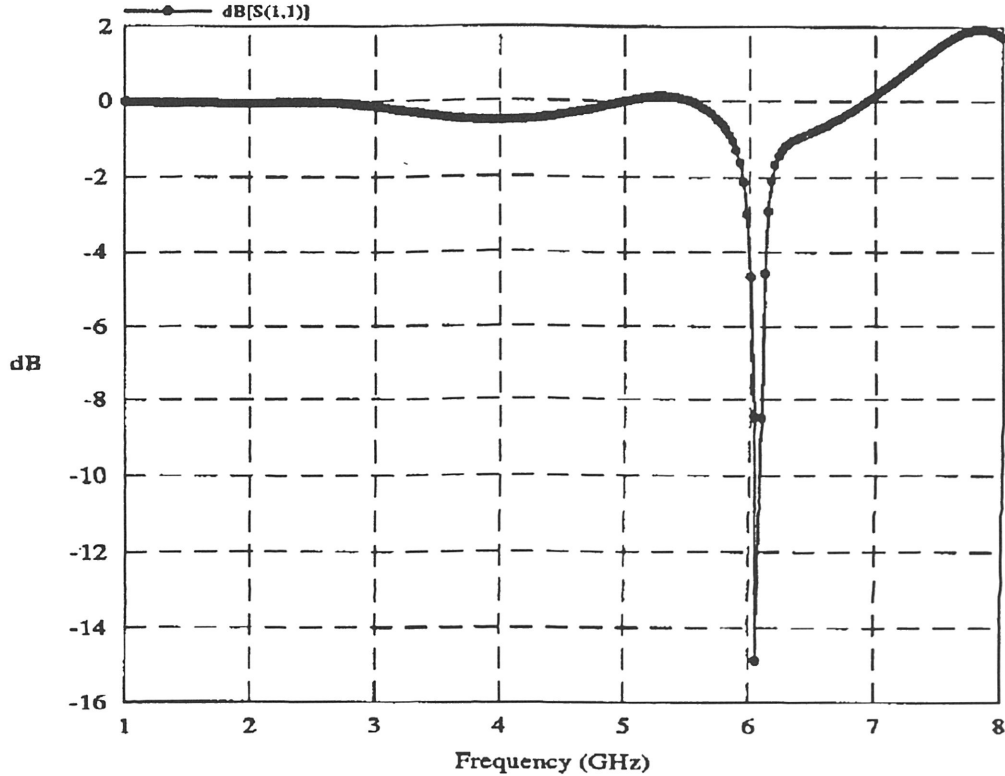


Figure 8. Theoretical Return Loss obtained from *IE3D* simulation..

C. Antenna testing.

Antenna tests include bandwidth (2:1), isotropic gain, and far field radiation pattern measurements. The 2:1 bandwidth is defined as the frequency range for which the antenna terminal voltage standing wave ratio (VSWR) equals 2. VSWR equal to 2 corresponds to 10% of the power being reflected from the antenna input terminal. The proof is given below [19].

$$VSWR = 2 \quad (13),$$

$$|\Gamma| = \frac{VSWR - 1}{VSWR + 1} = \frac{1}{3} \quad (14),$$

$$P_r = |\Gamma|^2 P_{IN} = \frac{1}{9} = 10.1\% \quad (15),$$

where P_{IN} is the power input to the antenna, and Γ is the reflection coefficient.

VSWR is measured using an HP8510 network analyzer and the two frequencies for which the VSWR equals 2 is the bandwidth. A general description of the ring bandwidth can also be determined from the return loss, S_{11} , measurement. Figure 8 shows a simulated return loss measurement using *IE3D*.

Far field radiation pattern and antenna gain measurements require more equipment and special environment considerations for accurate testing. These parameters can be tested outdoors or indoors, but the ideal test site prevents any external electromagnetic emanations from disturbing the measurement. An outdoor site must be large enough for the test antennas to be in the far field. The area close to the antenna stores reactive energy and is very susceptible to external influences such as metal objects. Also, the antennas are typically operated at far distances so the near field is not considered. For the purposes of this thesis, far field radiation pattern is synonymous with radiation pattern. Additionally, the test site must be clear of obstacles

that could return reflections from the RF test source and be far enough away from other transmission sources that operate in the same frequency band as the test antenna. Indoor antenna sites, or anechoic chambers, are metal enclosed chambers that prevent any external emanations from entering the test site. Additionally, the interior chamber walls are lined with electromagnetic absorbing materials that nearly eliminate reflections from the test RF sources.

The equipment used to test the antenna include a transmitting source, a power meter, and a standard reference antenna. The indoor chamber used in this study used an HP437 Power Meter, an HP 83622A Synthesized RF Sweeper as the transmitter source, and a Narda 612A C-Band Standard Horn Antenna. Figure 9 shows the set-up of the small anechoic chamber that was used for the test.

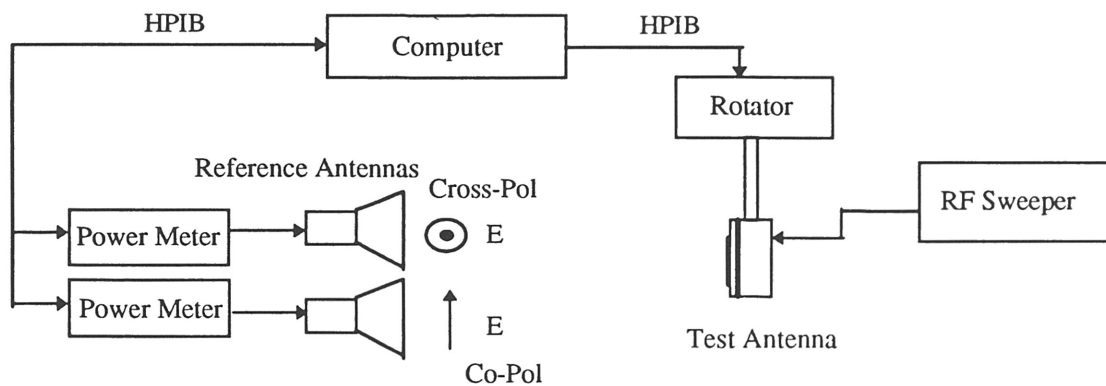


Figure 9 Antenna radiation pattern test set-up.

The test antenna is mounted on a positioner that rotates the antenna. The positioner is computer controlled and the RF sweeper is manually set to the frequency of interest. The power meters and standard antennas monitor the received power level which is sent to the computer for plotting purposes.

The E and H planes are the two principal planes for measuring the radiation patterns and are perpendicular to each other. In order to measure both planes the test antenna is rotated 90 degrees about the line of sight axis to the reference antennas. When the test antenna's electric field (E-field) is aligned with the reference antenna's E-field, the antennas are polarized in the same direction. The measurement is called the co-polarization (co-pol) measurement. When the E-fields are not polarized the measurement is called the cross-polarization (cross-pol) measurement. Two reference antennas are used to measure the cross-pol and the co-pol at the same time. This introduces a small error to the pattern measurement called skewing. Skewing is the tendency of the radiation pattern to be asymmetrical around line of sight axis, or boresight.

Gain measurements are performed with a similar test set-up. Instead of rotating the antenna throughout the measurement, the antenna is kept fixed while the frequency is swept through the operational bandwidth of the reference antenna. After the power radiation pattern for the test antenna is measure, the test antenna is rotated to the position where the least polarization error occurred and the frequency is swept. The receiver unit measures the power received and compares the test antenna to the reference antenna. The reference antenna is a standard that has been compared to an ideal isotropically radiating antenna. The gain, in dB, is calculated by equation (16), [5].

$$G_{dB} = 10 \log \left(\frac{P_{test}}{P_{ref}} \right) \quad (16),$$

where P is the power in milliwatts.

The difference with an active antenna measurement is that there is no RF source used with the transmit antenna because the source is on the antenna. The pattern measurements are still performed the same way because the pattern is independent of power, but the gain measurement

is performed using the Friis transmission equation. The simplified form that assumes impedance matched ports, zero polarization loss, and zero insertion loss due to cables and connectors is given in equation (17), [20].

$$P_t = P_r \left(\frac{4\pi R}{\lambda_o} \right)^2 \left(\frac{1}{G_r G_t} \right) \quad (17),$$

where P_t is the transmitted power in milliwatts, P_r is the received power in milliwatts, R is the separation distance in meters, λ_o is the free space wavelength in meters, and G_r and G_t are the respective unitless gains of the reference and test antennas. Solving equation (17) for G_r , as shown in (18), gives a quick calculation of the active antenna's gain.

$$G_t = P_r \left(\frac{4\pi R}{\lambda_o} \right)^2 \left(\frac{1}{G_r P_t} \right) \quad (18).$$

D. Experimental results.

The antenna design is shown in Appendix A. The mean radius of the ring is 2.885 mm, and was calculated using equation (3) - (6). The width of the microstrip feed line and the microstrip line for the ring have are 1.855 mm, corresponding to a 50 ohm characteristic impedance. The coupling gap was arbitrarily set to 0.3 mm.

The antenna's resonant frequency was tested with the HP8510 Network Analyzer. S_{11} was measured for a microstrip ring antenna, Figure 10. The high return loss (small value of S_{11}) shows a good impedance match between the network analyzer and the test antenna. This is important because the antenna and oscillator designs are referenced to 50 ohms so that when integrated into the same circuit they operate with minimal variation from the individual tests.

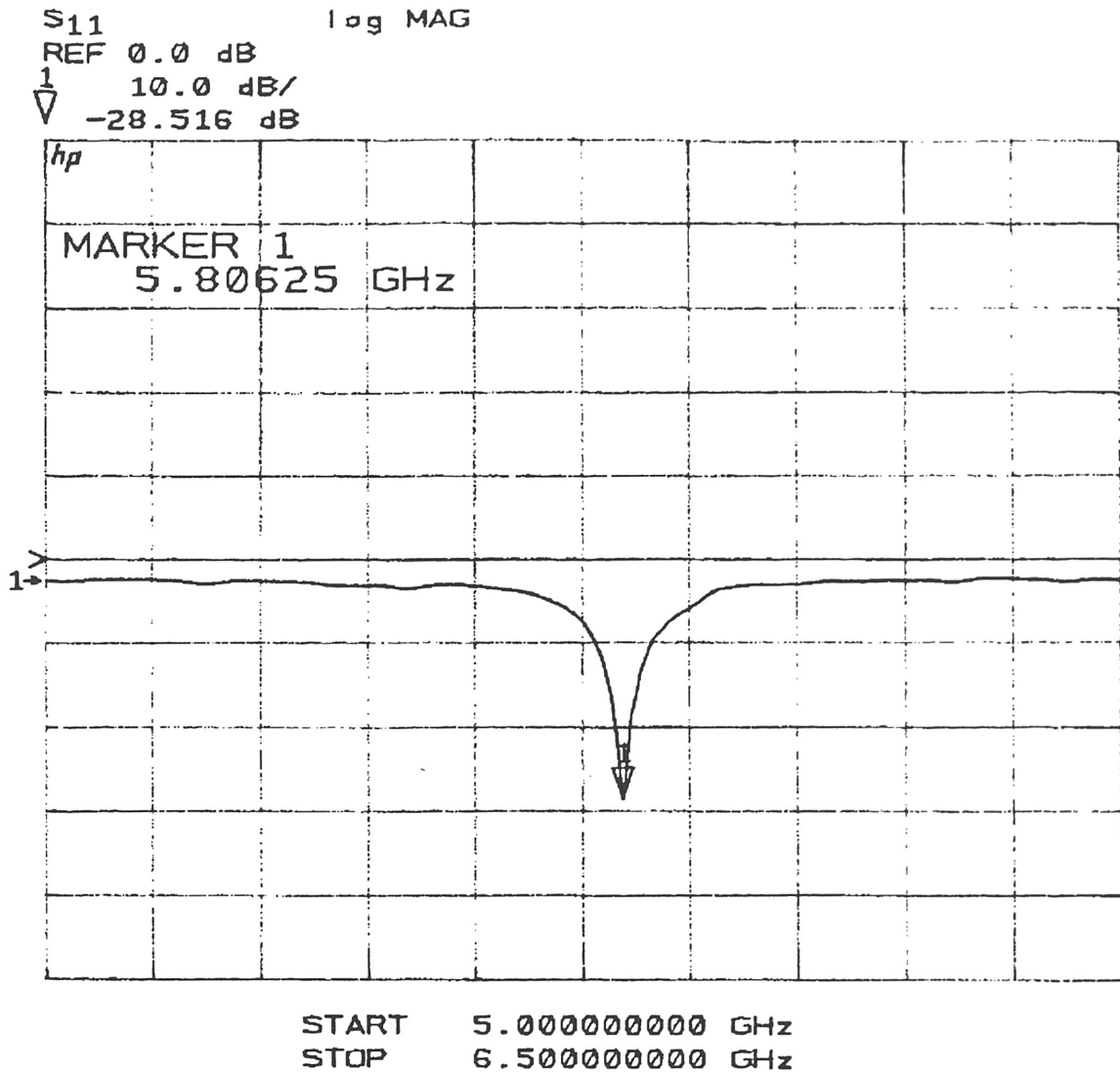
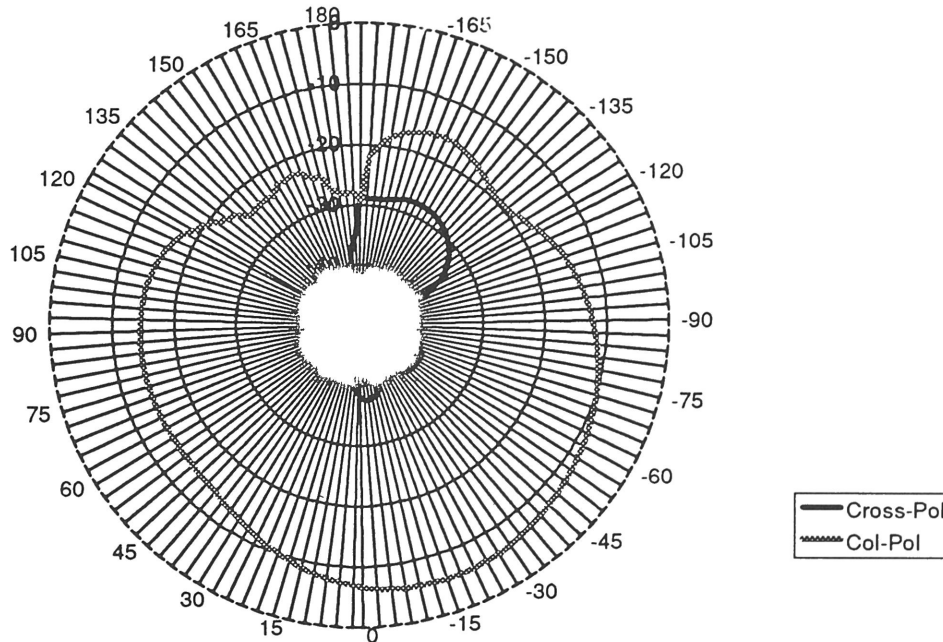


Figure 10. Measured return loss of microstrip ring antenna.

The radiation pattern in the E and H planes were measured in a mini-anechoic chamber specially designed for active antennas and millimeter wave applications. Figure 11 shows the E and H -plane radiation patterns. The ring antenna demonstrated a good H-plane pattern with a 80 degrees 3dB beamwidth and a maximum cross-pol level -18dB down from co-pol. The E-plane 3dB beamwidth is 75 degrees with a cross -30 dB down from the co-pol level. The E and H-plane patterns are slightly skewed from boresight, which are contributed to the unbalanced

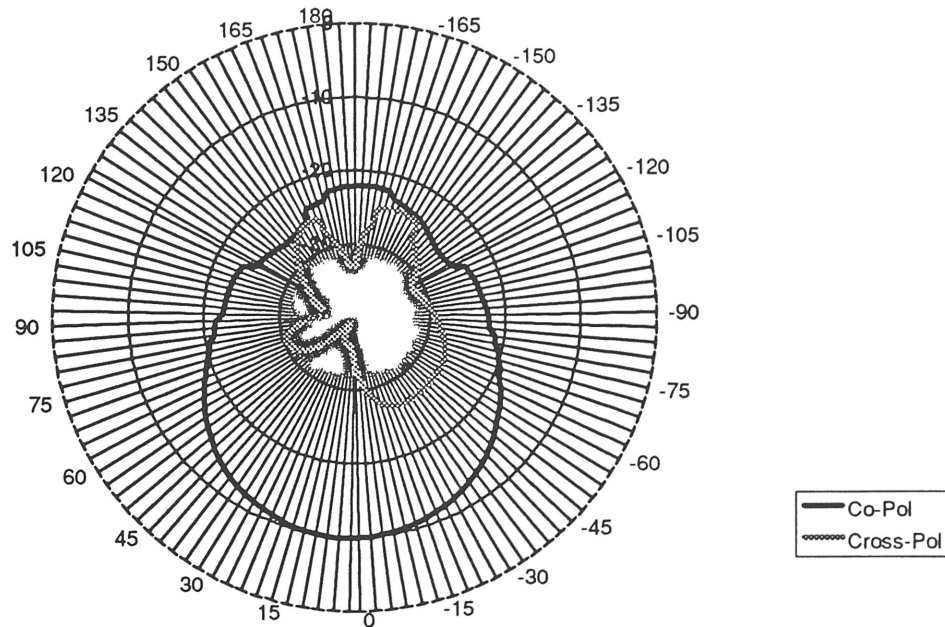
microstrip structure and the fact that the reference antennas were not directly on boresight. The antenna gain was not measured.

Passive Ring Antenna E-Plane



a) H-plane radiation pattern

Passive Ring Antenna H-Plane



b) E-plane radiation pattern

Figure 11. Radiation pattern a) H-plane b) E-plane

IV. Oscillator Design

A. Oscillator theory.

Oscillators convert direct current into alternating current at a particular frequency. There are different devices and circuit configurations for oscillators. Oscillators are designed as one or two port devices depending on the device used. Gunn diodes are two terminal devices used as one port oscillators, while FETs are three terminal devices used as two port oscillators. The transistor must be under certain conditions as shown in Figure 2, but the circuit configuration

ensures that those conditions are satisfied. There are three common transistor configurations used: common-drain, common-source, and common-gate. However, each type can use series feedback or shunt feedback [21]. Of the three configurations, the common-gate and the common-drain are used most commonly for microwave oscillators, while the common-source is used most often for amplifiers [22].

When a two port design is used, the FET is observed as shown in Figure 12, where Z is the impedance at the terminal and Γ is the reflection coefficient at the terminal [19].

The manufacturer's published S-parameters are used to design the terminating network and the load network. The terminating network is typically a resonant structure such as a microstrip open stub. If the input port of the transistor is not matched, then the S-parameters will not be valid for designing the load network. The load network must satisfy the oscillation conditions presented in section II.

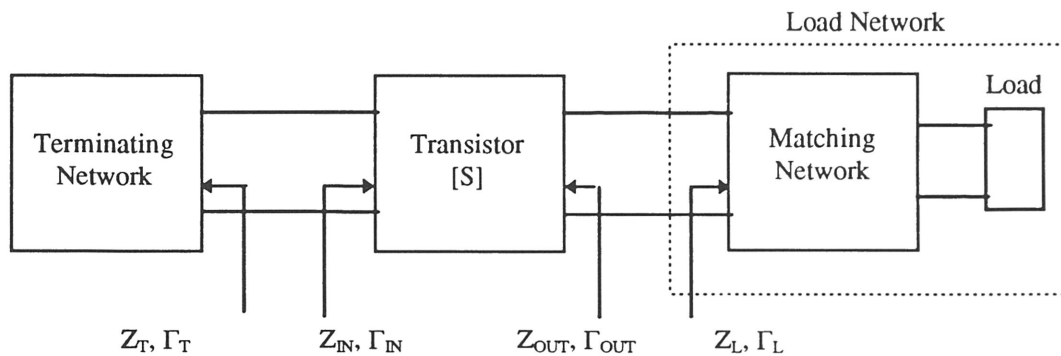


Figure 12. Two port oscillator design model.

However, FETs must exhibit the additional characteristic of instability. The unstable nature of the transistor is what allows it to begin oscillation. Random noise fluctuations begin

when DC power is applied. The resonant structure tunes the noise to the resonant frequency, and oscillations begin. Unstability of the FET is determined from the S-parameters according to equation (19).

$$K = \frac{1 - |S_{11}|^2 - |S_{22}|^2 + |\Delta|^2}{2|S_{12}S_{21}|} < 1 \quad (19),$$

where K is the stability factor and must be less than one for possible instability and $\Delta = S_{11}S_{22} - S_{12}S_{21}$. If the device is stable, then oscillation will not occur. The device can be made unstable by adding feedback or using another common configuration.

To ensure oscillation one needs to keep the load resistance less than the absolute value of the FET's output resistance [19]. Typically the load resistance is designed by

$$R_{Load} \leq \frac{1}{3} |R_{Out}| \quad (20)$$

This ensures that the first oscillation condition of section II is satisfied in spite of circuit fabrication variations, and DC biasing fluctuations.

B. Oscillator testing.

Oscillator tests include frequency, power output, stability, and phase noise. Each of these can be measured with a modern spectrum analyzer and power meter. The frequency is measured with the accuracy of the spectrum analyzer's internal clock, which is typically on the order of 10^{-7} Hz. A power meter can be used to measure average power which includes all harmonic power, but the fundamental frequency is only of concern, so a spectrum analyzer is used to measure the peak fundamental frequency power. The stability is checked by setting the spectrum analyzer's display controls for a narrow frequency span. This provides enough resolution for the observer to determine how well the oscillator's frequency remains stable. Also, with the resolution bandwidth

controls, one can measure the phase noise. Phase noise is a measure of random noise, harmonics, and frequency fluctuation power. A resolution bandwidth of 30 kHz is often used to determine how much power is in the phase noise up to 100 kHz above and below the fundamental frequency.

C. Oscillator experiments.

The oscillator was designed for a common gate configuration. The design and simulation code are shown in Appendix B. The substrate used was Duroid 6010 with a thickness of 50 mils and $\epsilon_r = 10.5$. Two port design techniques as described in section IV. A. were employed for an initial design, and then *Libra* [23], a well known microwave circuit simulator, was used to optimize the circuit for the DC bias scheme. Two FETs were used: a Hewlett-Packard ATF-26836 general purpose Gallium Arsenide (GaAs) FET, and an NEC NC76184AS general purpose GaAs FET. Both FETs were operated at 2.0 V with a $V_{GS} = 0$ V. The NEC FET operated at considerably less current (55 mA) than the HP FET (140 mA).

The *Libra* simulation was used to show the oscillator's output impedance vs. frequency so that the resonant frequency could be determined. Figure 13 shows the *Libra* generated impedance plot for the oscillator's output port.

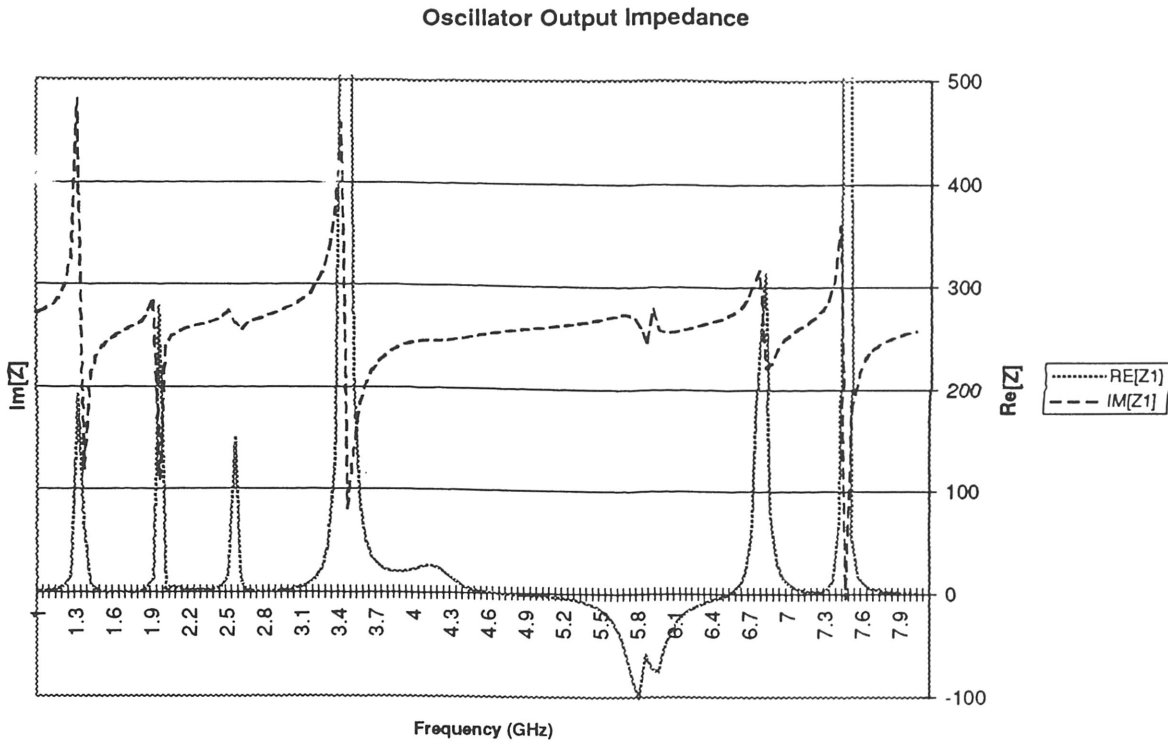


Figure 13. Oscillator output impedance from *Libra* simulation.

The resistance is negative (-75 ohms) and the reactance is equal to zero at 5.8 GHz, so the second oscillation condition from section II is satisfied. The oscillator also has a larger value of negative resistance as compared to a standard 50 ohm load, so oscillation can occur. Recall that the antenna measurement demonstrated a very good impedance match to 50 ohms, so the second condition for oscillation given in section II is also satisfied.

The measured oscillator frequency and relative harmonics are shown in Figure 14.

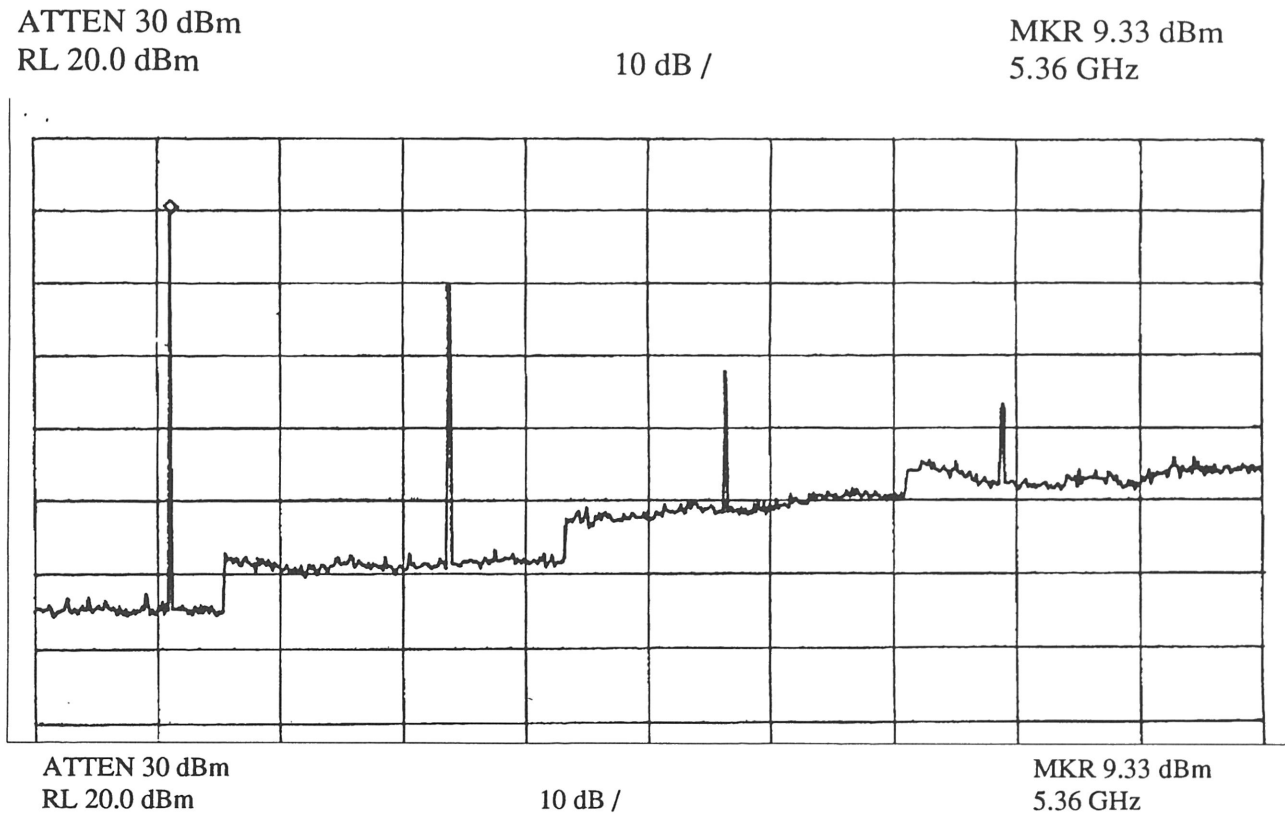


Figure 14. Measured oscillator power spectrum.

The fundamental frequency is 5.36 GHz with 9.33 dBm peak power. This is a 7.59% difference from the design frequency. Tuning was done by adding the tweaking pads (extra lengths of microstrip transmission line, see Appendix B) to the gate and source open microstrip stubs. The peak power of the fundamental was good and the efficiency was good (10.30%). RF efficiency is calculated by

$$\eta \% = \frac{P_{RF}}{P_{DC}} \times 100 = 10.30\% \quad (21),$$

$$P_{DC} = I_{DC} V_{DC} \quad (22),$$

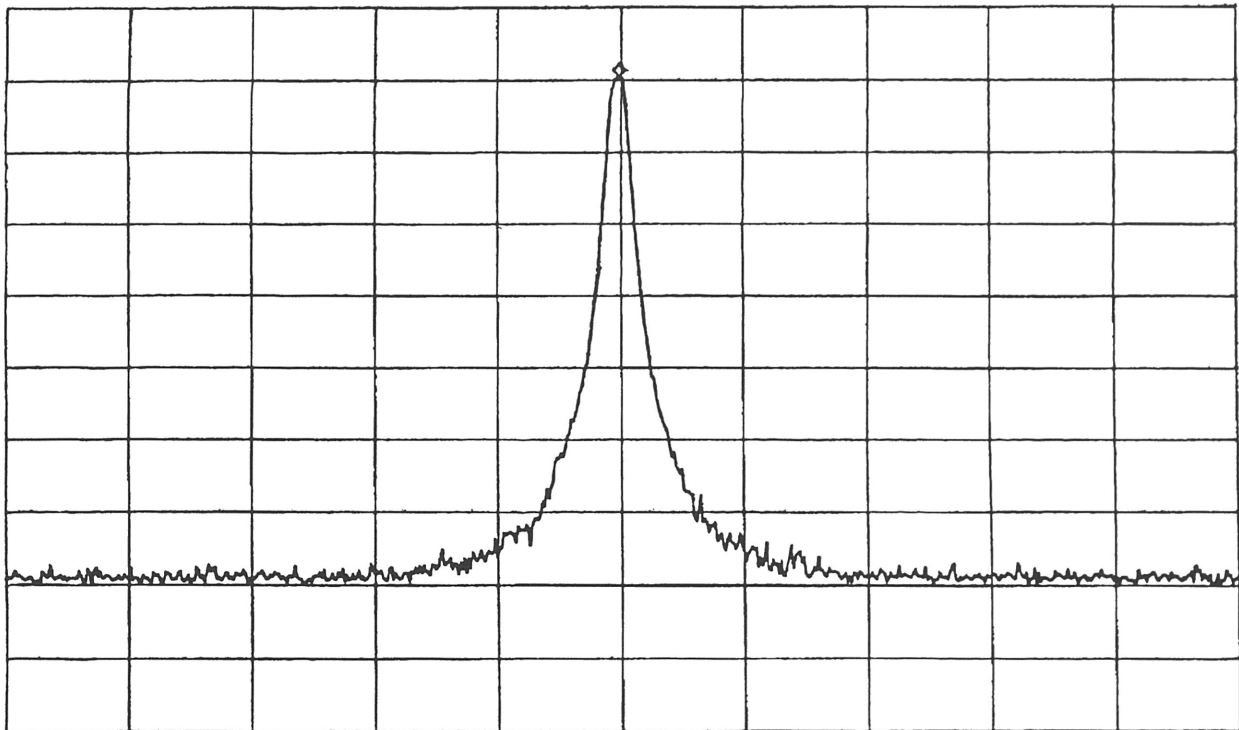
where $\eta\%$ is the RF efficiency in percent, and P is power in mW, V = 2.0 volts, and A = 140 mA.

The oscillator design does not use a resonator in the circuit, and subsequently the oscillator is not very stable at the frequency. Subsequent designs planned to use a microstrip ring resonator to improve the stability. Figure 15 shows the fundamental frequency with a 5 MHz resolution bandwidth. The phase noise was not measured because the fundamental frequency was not stable enough to accurately measure the phase noise power within 100 kHz.

ATTEN 30 dBm
RL 20.0 dBm

10 dB /

MKR 10.33 dBm
5.356823 GHz



CENTER 5.356832 GHz
RBW 30 kHz

VBW 30 kHz

SPAN 5.000 MHz
SWP 50 ms

Figure 15. Measured fundamental frequency stability.

The oscillation frequency was not at the correct frequency because the simulation code that was used had an error. The code uses the manufacturer's published S-parameters as a two

port network, however, the design simulation should have been performed using 3 port S-parameters. Therefore the plot for the oscillator output impedance was incorrect and the design lengths for the microstrip circuit were incorrect.

An additional design flaw was the DC bias network for the FET drain terminal. The current design reduced the efficiency because some of the RF energy went to the DC bias line instead of to the output port. The efficiency can be improved by placing a radial open stub where the bond pad (see circuit layout in Appendix B) is and moving the bond pad via another bias line. The bias should be similar to the source and gate bias lines.

The simulation code error was verified by using the 3 port S-parameters in the same simulation code, and the results predicted the experimental results.

V. Integrated Active Antenna Results

A. Integrated active antenna measurements.

Active antennas test the same parameters as passive antennas, but also include additional tests for the active components. Typical tests include: spectrum quality, stability, noise, radiation pattern, and conversion efficiency. The spectrum, quality, and stability, and noise tests are performed with a spectrum analyzer, similar to an oscillator [5]. Radiation pattern measurements are performed similar to the passive antenna with the exception of the external RF source. The set-up in Figure 9 is still used, however, the RF source is now on the antenna. This creates a difficulty with measuring the power from the oscillator because any special test connections built into the active antenna can affect the radiation power pattern. Navarro and Chang, [5], suggest

using the equivalent isotropic radiated power (EIRP) as a figure of merit for the active antenna. EIRP is the amount of power transmitted by an isotropic radiator given the received power.

$$EIRP \equiv P_t G_t = \frac{P_r}{G_r} \left(\frac{4\pi r}{\lambda} \right)^2 \quad (24),$$

where P is in mW, G is the gain as a ratio, r is the separation distance between the test antenna and the standard horn antenna, and λ is the free space wavelength. The received power is measured with the active antenna aligned for maximum power received.

The integrated active antenna was not tested because of the oscillator design hindrances. It is important for the oscillator to be at the correct operating frequency because integrated active antenna oscillators do not have any protection circuits against returned signals. Normally, an oscillator is followed by a bandpass filter. The filter eliminates most of the harmonic frequencies that are present at the oscillator output. Filters are commonly made to be reciprocal networks, so that any affect on signal propagation in one direction also happens to signals propagating in the opposite direction, i.e. any returned harmonics that pass through the filter and return, are reduced in power even further.

In addition, the oscillator is not expected to work with the antenna at another frequency. As reference to Figure 10, the antenna exhibits high return loss at 5.36 GHz, so any signal at the antenna would be severely attenuated and may not be measurable.

Another oscillator has been designed and will be fabricated at the time this thesis is reviewed. It will take approximately one week to fabricate and test the circuit, at which time the results will be amended to this thesis.

VI. Conclusions

The intent of this study was to design a RFID FET based integrated active antenna. The experimental approach to the design for this novel idea was partially successful. A passive ring antenna, suitable for RFID tags, has been developed. The antenna demonstrates wide symmetrical beamshape (>70 degrees) with low cross-pol levels (<-18 dB down). Also, the antenna exhibited very low return loss (-28 dB) indicating that it will provide a good match to an appropriately matched oscillator.

The oscillator design frequency was not reached with the design, but the design flaw was identified and is being corrected for inclusion with the amendment to this thesis. Positive aspects of the FET oscillator are higher dc-to-rf efficiency than Gunn diodes. This is the most important parameter for RFID tags because the tags are battery operated. The modest 10.30% efficiency can be improved further with slight modifications to the dc bias scheme, but will also improve with the continuing improvements in FET fabrication. Furthermore, the microstrip structure is ideal because lumped elements (capacitors and inductors) are not needed, since they are substituted with microstrip lines using transmission line theory.

Once the oscillator is integrated with the microstrip ring antenna, some degradation of the ring antenna's performance is expected to occur. Also, the oscillator may require post fabrication tuning since it can not be analyzed separately once integrated with the antenna. Further research to fabricate and test this new application of active antennas is needed.

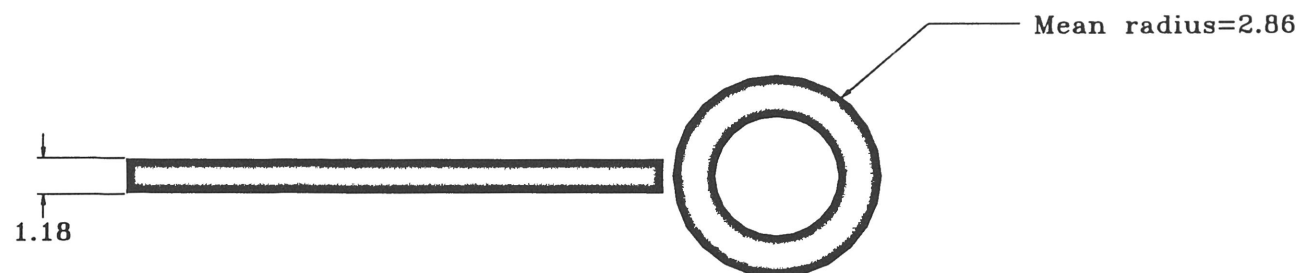
REFERENCES

- [1] J. Eagleson, "Matching RFID Technology to Wireless Applications," *Wireless Systems Design*, pp. 41-48, May 1996.
- [2] R. Schneiderman, "RFID Equipment Manufacturers Struggle With Standards," *Wireless Systems Design*, pp. 12-14, October 1996.
- [3] Micron Web Page, "RIC vs. RFID," Micron Communications Inc., October 31, 1996.
- [4] J. R. Tuttle, B. A. Pier, "New Technology EXPANDS RFID Applications," *Wireless Systems Design*, pp. 24-27, October 1996.
- [5] J. Navarro, K. Chang, Integrated Active Antennas and Spatial Power Combining, John Wiley & Sons, Inc., 1996.
- [6] J. Birkeland, T. Itoh, "FET-Based Planar Circuits for Quasi-Optical Sources and Transceivers," *IEEE Trans. on Microwave Theory and Techniques*, Vol. 37, No. 9, pp. 1452-1459, December 1989.
- [7] J. Lin, T. Itoh, "Active Integrated Antennas," *IEEE Trans. on Microwave Theory and Techniques*, Vol. 42, No. 12, pp. 2186-2194, December 1994.
- [8] C. Montiel, L. Fan, K. Chang, "A Novel Active Antenna with Self-Mixing and Wideband Varactor Tuning Capabilities for Communication and Vehicle Identification Applications," *IEEE Trans. on Microwave Theory and Techniques*, Vol. 44, No. 12, pp. 2421-2430, December 1996.
- [9] R. Flynt, L. Fan, J. Navarro, K. Chang, "Low Cost and Compact Active Integrated Antenna Transceiver for System Applications," *IEEE Trans. on Microwave Theory and Techniques*, Vol. 44, No. 10, pp. 1642-1649, October 1996.
- [10] J. Bartolic, D. Bonafacic, Z. Sipus, "Modified Rectangular Patches for Self Oscillating Active Antenna Applications," *IEEE Antennas and Propagation Magazine*, Vol. 38, No. 4, pp. 13-21, August 1996.
- [11] C. W. Pobanz, T. Itoh, "A Microwave Noncontact Identification Transponder Using Subharmonic Interrogation," *IEEE Trans. on Microwave Theory and Techniques*, Vol. 43, No. 7, pp. 1673-1679, July 1995.
- [12] C. -H. Ho, L. Fan, K. Chang, "New FET Active Slotline Ring Antenna," *Electronic Letters*, Vol. 29, No. 6, pp. 521-522, March 18, 1993.

- [13]K. Chang, Microwave Ring Circuits and Antennas, John Wiley & Sons, Inc., 1996.
- [14]LINECALC, EEsof Inc., Westlake Village, Calif.
- [15]M. Kirshing, R.H. Jansen, "Accurate model for effective dielectric constant of microstrip and validity up to millimeter-wave frequencies," *Electron. Lett.*, Vol. 18, pp. 272-273, March 1982.
- [16]A. K. Bhattacharyya, R. Garg, "Input Impedance of annular ring microstrip antenna using circuit theory approach," *IEEE Trans. Antennas Propagation*, Vol. AP-33, No. 4, pp. 369-374, April 1985.
- [17]A. K. Bhattacharyya, R. Garg, "Self and mutual admittance between two concentric, coplanar, circular radiating current sources," *Proc. IEE*, Vol. 130, Pt. H, No. 6, pp.217-219, June 1984.
- [18]IE3D, Zeland Software Inc., Fremont Calif.
- [19]K. Chang, Microwave Solid State Circuits and Applications, John Wiley & Sons, Inc., 1994.
- [20]W. L. Stutzman, G. A. Thiele, Antenna Theory and Design, John Wiley & Sons, Inc., 1981.
- [21]S. Liao, Microwave Circuit Analysis and Amplifier Design, Prentice-Hall, Inc., 1987.
- [22]A. S. Khanna, "Three-port S-parameters ease GaAs FET designing," *Microwaves and RF*, pp. 81-84, Nov. 1985.
- [23]Libra, EEsof Inc., Westlake Village, Calif.

APPENDIX A- Microstrip Ring Antenna Drawing.

Ring Drawing

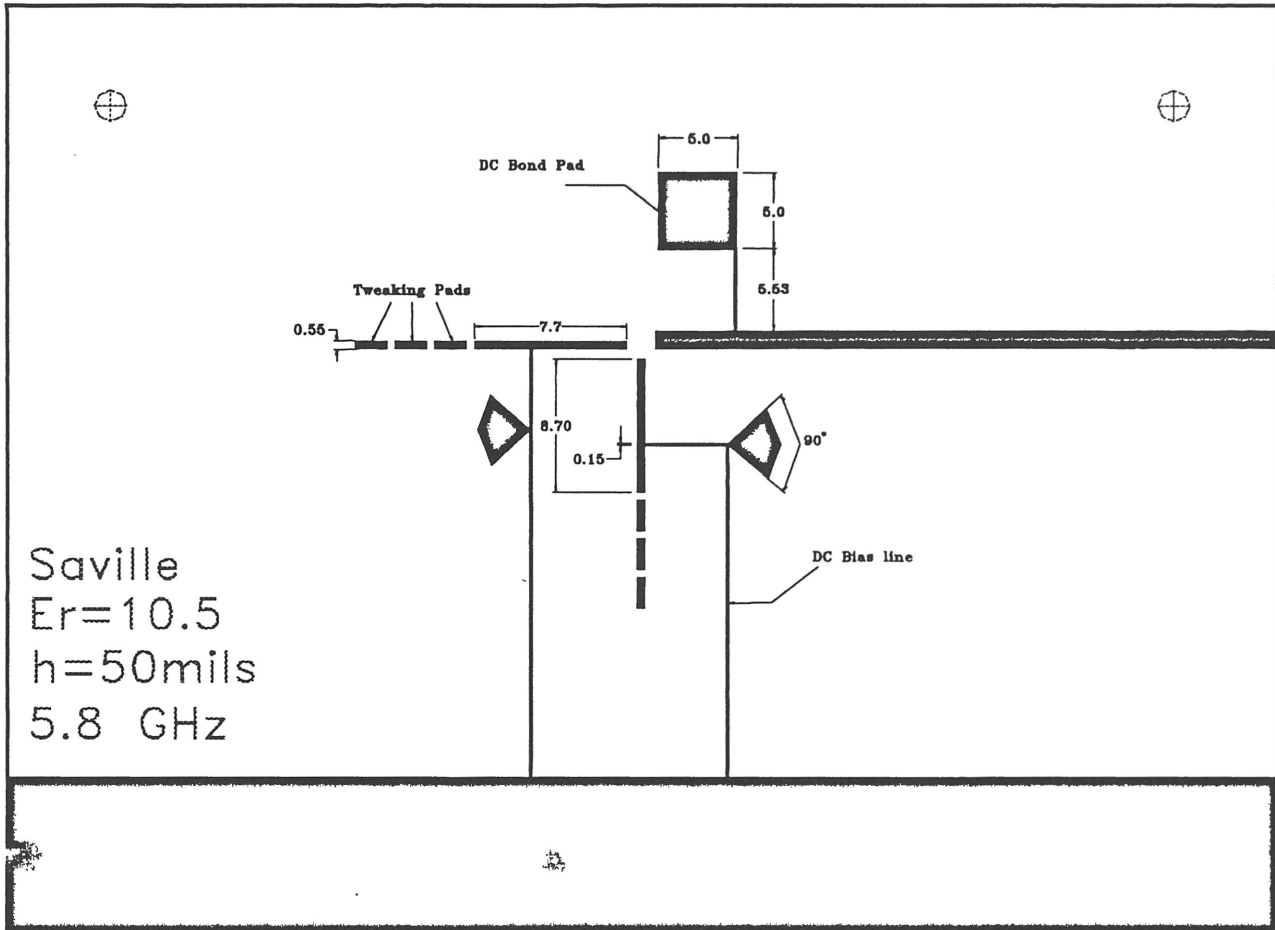


Note: All dimensions are in mm.

The substrate is 6010 with a dielectric constant of 10.5, and the substrate height is 1.524 mm.

APPENDIX B - Oscillator Drawing and Libra Source File

Circuit Drawing



Note: All dimensions are in mm.

Substrate height is 1.524 mm, and the relative dielectric constant is 10.5.

Libra Circuit File for Oscillator.

```
! FILENAME:FETOSC1.CKT VERSION:1.0  DATE:FEB 1, 1997  19:38:43
!
! MODIFICATIONS
! -----
! VERSION DATE  TIME PROGRAMMER  DESCRIPTION
! 1.0 02/01/1997 19:38:43 SAVILLE  5.8 GHZ FET OSCILLATOR
!
! $NOKEYWORDS$
!
! DESCRIPTION
! -----
! FILENAME: FETOSC1.CKT
! PURPOSE : DESIGN FET OSCILLATOR
! DATE   : 2/01/97
```

```
DIM
FREQ GHZ
RES OH
COND /MOH
CAP PF
IND NH
ANG DEG
VOL V
CUR MA
PWR DBM
TIME NS
LNG MM
```

VAR

```
L1 # 5 9.9183 10 ! gate open stub
L1A # .1 6.99744 10 ! gate second section
L2 # 2 3.94858 4 ! source open stub start section
L3 # 2 3.10997 4 ! source stub mid section
L4 # 2 3.31229 4 ! source stub end section
LBias # 3 4.83723 7 ! bias line length
LRstub # 3 3.71395 7 ! radial stub radius
WBias = .1 ! bias line width
WStub # .5 0.599997 1 ! open stub line widths
```

CKT

```
MSUB ER=10.5 H=1.27 T=.025 RHO=1 RGH=0
S3P_AOSC 1 2 3 C:\USER\MICHAEL\Nec76184.S3P
```

```
MLIN 1 4 W^WStub L^L1 ! Gate open stub
MLOC 4 W^WStub L^L1A
```

```
MLIN 4 10 W^WBias L^LBias ! Gate bias line
MRSTUB_GND 10 W^WBias L^LRstub ANG=90
MLSC 10 W^WBias L=10
```

```
MLIN 3 5 W^WStub L^L2 ! Source open stub
MLIN 5 6 W^WStub L^L3
MLOC 6 W^WStub L^L4
```

```
MLIN 6 21 W^WBias L^LBias ! Source bias line
MRSTUB_GND 21 W^WBias L^LRstub ANG=90
MLSC 22 W^WBias L^LBias
MCORN 21 22 W^WBias
```

```
MLIN 2 8 W=1.18 L=5 ! Drain port
MLIN 8 50 W=1.18 L=10
```

```
MLIN 8 31 W^WBias L^LBias ! Drain bias
MRSTUB_VDD 31 W^WBias L^LBias ANG = 90
MLIN 32 40 W^WBias L^LBias
MCORN 31 32 W^WBias
MLOC 40 W=5 L=5
MSTEP_VDD 30 40 W1=5 W2^WBias
```

```
DEF1P 50 OSC1
```

```
SOURCE
OSC1 VS_VDD 40 0 DC=2 ! DRAIN BIAS
```

```
OUT
OSC1 RE[Z1] GR1
OSC1 IM[Z1] GR1A
```

```
FREQ
SWEEP 1 8 .05 ! LINEAR FREQUENCY SWEEP
```

```
GRID
FREQ 1 8 1 ! LINEAR FREQUENCY DISPLAY RANGE
GR1 -75 25 15 ! RE[Z1] SCALE
GR1A -12 12 ! IM[Z1] SCALE
```

```
HBCNTL
RELTOL = 1E-8
SAMPLE = 2
```

```
OPT
FREQ 1 5.5 .1
OSC1 RE[Z1] >0 10
```

```
FREQ 5.6 6 .01
OSC1 RE[Z1] <-50 9
```

```
FREQ 5.799 5.801 .001
OSC1 IM[Z1] = 0 8
```